Inflammatory Bowel Diseases

Separation of dual oxidase 2 and lactoperoxidase expression in intestinal crypts and species differences may limit hydrogen peroxide scavenging during mucosal healing in mice and humans

--Manuscript Draft--

Manuscript Number:	
Article Type:	Original Research Articles - Basic Science
Keywords:	Host defence; Doux2; hydrogen peroxide; thiocyanate; gut pathogens; colitis.
Corresponding Author:	andy silver ICMS London, United Kingdom
First Author:	Alice Rigoni
Order of Authors:	Alice Rigoni
	Poulsom Richard
	Rosemary Jeffery
	Shameer Mehta
	Amy Lewis
	Christopher Yau
	Eleni Giannoulatou
	Roger Feakins
	James Lindsay
	Mario Colombo
	andy silver
Manuscript Region of Origin:	UNITED KINGDOM
Abstract:	Background: DUOX2 and DUOXA2 form the predominant H2O2-producing system in human colorectal mucosa. Inflammation, hypoxia, and 5-aminosalicylic acid increase H2O2 production supporting innate defense and mucosal healing. Thiocyanate reacts with H2O2 in the presence of lactoperoxidase (LPO) to form hypothiocyanate (OSCN-), which acts as a biocide and H2O2 scavenging system to reduce damage during inflammation. We aimed to discover the organization of Duox2, Duoxa2 and Lpo expression in colonic crypts of mice, and how distributions respond to Dextran Sodium Sulphate (DSS)-induced colitis and subsequent mucosal regeneration. Methods: we studied tissue from DSS exposed mice and human biopsies using in situ hybridisation, Reverse Transcription-quantitative PCR and cDNA microarray analysis. Results: Duox2 mRNA expression was mostly in the upper crypt quintile whilst Duoxa2 was more apically-focused. Most Lpo mRNA was in the basal quintile, where stem cells reside. Duox2 and Duoxa2 mRNA were increased during the induction and resolution of DSS colitis, whilst Lpo expression did not increase during the acute phase. Patterns of Lpo expression differed from Duox2 in normal, inflamed and regenerative mouse crypts ($p < 0.001$). We found no evidence of LPO expression in human gut. Conclusions: The spatial and temporal separation of H2O2-consuming and -producing enzymes enables a thiocyanate- H2O2 'scavenging' system in murine intestinal crypts to protect the stem/proliferative zones from DNA damage, while still supporting higher H2O2 concentrations apically to aid mucosal healing. The absence of LPO expression in human gut suggests an alternative mechanism or less protection from DNA damage during H2O2 driven mucosal healing.

Separation of dual oxidase 2 and lactoperoxidase expression in intestinal crypts and species differences may limit hydrogen peroxide scavenging during mucosal healing in mice and humans

Alice Rigoni, PhD,[*] Richard Poulsom DSc,[†] Rosemary Jeffery, HNC,[†] Shameer Mehta, MRCP,[†] Amy Lewis, PhD,[†] Christopher Yau, DPhil,[‡§] Eleni Giannoulatou, DPhil [‖¶], Roger Feakins, FRCPath[**], James O Lindsay, PhD[††], Mario P Colombo, PhD,[*] Andrew Silver, PhD,[†]

[*]Molecular Immunology Unit, Department of Experimental Oncology and Molecular Medicine, Fondazione IRCCS Istituto Nazionale dei Tumori, Milan, Italy; [†]Centre for Genomics and Child Health, Blizard Institute, Barts and The London School of Medicine and Dentistry, Queen Mary University of London, London UK; [‡]The Wellcome Trust Centre for Human Genetics and [§]Department of Statistics, University of Oxford, Oxford UK; [‖]Victor Chang Cardiac Research Institute, Sydney, NSW 2010, Australia and [¶]St Vincent's Clinical School, University of New South Wales, Sydney, NSW 2052, Australia; [**]Department of Histopathology, The Royal London Hospital, London UK; [††]Centre for Immunobiology, Blizard Institute, Barts and The London School of Medicine and Dentistry, Queen Mary University of London, London UK

AR, RP and RJ contributed equally to this work

*_Correspondence to:_ Professor Andrew Silver, PhD, Centre for Digestive Diseases, Blizard Institute, Barts and The London School of Medicine and Dentistry, 4 Newark St, Whitechapel, London E1 2AT UK. Phone: +44 (0)20-7882-2590. Email: a.r.silver@qmul.ac.uk

CONFLICTS OF INTEREST STATEMENT

The authors have no conflicts of interest to disclose.

Key Words: Host defence, hydrogen peroxide, thiocyanate, gut pathogens, colitis.

Abbreviations used: Advanced Cell Diagnostics, ACD; Colorectal cancer, CRC; Crohn's disease, CD; Dextran Sodium Sulphate, DSS; dual oxidase, DUOX; formalin-fixed paraffin-embedded, FFPE; Glutathione Peroxidase, GPX; hypothiocyanate, $OSCN^-$; immunohistochemistry, IHC; inflammatory bowel disease, IBD; *in situ* hybridisation, ISH; Lactoperoxidase, LPO; Reverse Transcription-quantitative PCR, RT-qPCR; reactive oxygen species, ROS; Ulcerative colitis, UC.

ABSTRACT

Background: DUOX2 and DUOXA2 form the predominant H2O2-producing system in human colorectal mucosa. Inflammation, hypoxia, and 5-aminosalicylic acid increase H_2O_2 production supporting innate defense and mucosal healing. Thiocyanate reacts with H_2O_2 in the presence of lactoperoxidase (LPO) to form hypothiocyanate (OSCN-), which acts as a biocide and H_2O_2 scavenging system to reduce damage during inflammation. We aimed to discover the organization of *Duox2, Duoxa2* and *Lpo* expression in colonic crypts of mice, and how distributions respond to Dextran Sodium Sulphate (DSS)-induced colitis and subsequent mucosal regeneration.

Methods: we studied tissue from DSS exposed mice and human biopsies using *in situ* hybridisation, Reverse Transcription-quantitative PCR and cDNA microarray analysis.

Results: *Duox2* mRNA expression was mostly in the upper crypt quintile whilst *Duoxa2* was more apically-focused. Most Lpo mRNA was in the basal quintile, where stem cells reside. *Duox2* and *Duoxa2* mRNA were increased during the induction and resolution of DSS colitis, whilst Lpo expression did not increase during the acute phase. Patterns of Lpo expression differed from *Duox2* in normal, inflamed and regenerative mouse crypts ($p < 0.001$). We found no evidence of *LPO* expression in human gut.

Conclusions: The spatial and temporal separation of H_2O_2-consuming and -producing enzymes enables a thiocyanate- H_2O_2 'scavenging' system in murine intestinal crypts to protect the stem/proliferative zones from DNA damage, while still supporting higher H_2O_2 concentrations apically to aid mucosal healing. The absence of LPO expression in human gut suggests an alternative mechanism or less protection from DNA damage during H_2O_2 driven mucosal healing.

INTRODUCTION

Host defence and control of commensal bacterial populations in the gut of a broad range of species, including flies, fish and mammals, involves the dual oxidase enzyme (DUOX) acting in concert with its obligate maturation factor/partner encoded by an adjacent gene (DUOXA).[1,2] Recently, we reported that DUOX2/DUOXA2 form the predominant H_2O_2-producing enzyme system in human colorectal mucosa,[3] which is capable of releasing significant quantities of H_2O_2 from the epithelial layer into the gut lumen as part of the innate immune response. The DUOX2/DUOXA2 system is upregulated during bacterial infection and specifically during inflammatory bowel disease (IBD); the genes are regulated on a crypt-by-crypt basis in the colitic mucosa.[3] Loss of Duox2 activity in *Duoxa*$^{-/-}$ mice negates inflammatory response and permits gastric colonization by *Helicobacter felis,* highlighting the essential role of epithelial production of H_2O_2 in restricting microbial colonisation.[4]

H_2O_2 has significant toxicity, killing some pathogens at sub-milli-molar concentration, and has a relatively long half-life *in vivo* so that significant concentrations are achieved distant from external cell membranes by diffusion. However, pathogens such as *Campylobacter jejuni,*[5] *Helicobacter pylori,*[6] *Helicobacter hepaticus,*[7] and enterobacteriaceae family bacteria,[8] including *Escherichia coli*, *Shigella*, and *Salmonella* produce catalase to deactivate H_2O_2 allowing the pathogen to escape the host's innate immune response. Catalase activity is lower in colorectal cancer (CRC),[9] gastric adenocarcinoma, and *H. pylori*-infected stomach,[10] compared to normal tissues, and mononuclear cells of patients with Crohn's disease (CD) show suppressed catalase activity.[11] Colitis and colonic tumour burden in treated mice is reduced by oral administration of genetically modified catalase-proficient Lactobacilli.[12,13] Certain bacteria can stimulate a host's epithelial cells by releasing uracil, which at nano-molar

concentrations drives DUOX expression and H_2O_2 release.[14] Consequently, H_2O_2 is well suited to modulating the number and type of gut pathogens, which in turn can counter the host's response by altering the microenvironment to their advantage.

H_2O_2 can be reduced by a halide to produce a range of compounds with stronger biocidal effects. Thiocyanate (principally from dietary sources) reacts with H_2O_2 in the presence of the enzyme lactoperoxidase (LPO) to form the powerful broad-spectrum biocide hypothiocyanate ($OSCN^-$) that is effective against a wide range of bacteria, viruses, yeast and fungi.[15] These reactions also serve to consume H_2O_2, reducing the potential to damage host DNA through induction of single- and double-strand breaks.[16] In the respiratory tract DUOX1/DUOX1A are the principal producers of H_2O_2. Both are expressed, together with LPO, by subsets of cells within submucosal glands of airways, and protect the respiratory tract of mammals from pathogens. In cystic fibrosis the H_2O_2/thiocyanate/LPO system may be compromised due to mutation of the *CFTR* gene. The consequent reduced consumption of H_2O_2 then damages lung parenchyma.[17] It remains to be demonstrated that the H_2O_2/thiocyanate/LPO system is active in both human and mouse bowel.

Our recent study was the first to detail the site of expression of *DUOX2* and *DUOXA2* in human colorectal epithelium and show their relationship to inflammation and DNA damage.[3] Animal models of colitis might now offer a way to understand more clearly the regulatory pathways involved, their dynamics, and to test novel interventions. Colitis can be induced in mice in a number of ways, including exposure to dextran sodium sulphate (DSS) in the drinking water. The severity of the induced-colitis varies between mouse strains and the genetic basis is not well defined. Esworthy and colleagues used mice whose susceptibility to reactive oxygen species (ROS) was altered by deletion of

the Glutathione Peroxidase (GPX) 1 and GPX2 scavenging enzymes and quantitative trait loci mapping to identify genes that influence the severity of colitis.[18] They identified *Duox2* and *Duoxa2* organised on mouse Chromosome 2 in a head to head orientation as one of the top-ranked loci.[19] Susceptible and non-susceptible background mouse strains both expressed Lpo within epithelial cells of the gut mucosa, but with different immuno-staining intensity.[20] Thus the H_2O_2/thiocyanate/Lpo system is available in the mouse gut as well as lung. However, it remained to be seen if Duox2/DuoxA2 and Lpo are co-expressed in the normal intestine and/or during a DSS-induced inflammatory flare.

In this study, we sought to discover how *Duox2, Duoxa2* and *Lpo* expression is organised in colonic crypts of normal mice, and how these distributions respond to DSS colitis. The DSS colitis model is the most extensively use model of its type and has been reported on many times in the literature. For any given strain of mouse and at a particular dosage the model is highly reproducibility. We choose to focus our analysis of expression on substantial numbers of crypts within the colon. As there are no antisera available to demonstrate specifically Duox2 and Duoxa2 in formalin-fixed paraffin-embedded (FFPE) mouse tissues, we assessed mRNA distributions using highly specific and sensitive RNAscope® *in situ* hybridisation (ISH) to generate discrete signal dots from mRNA targets. This allowed us to observe precisely where *Duox2*, *Duoxa2* and *Lpo* were expressed normally and assess how they were modulated in inflammation and regeneration of ulcerated mucosa.

MATERIALS AND METHODS

Dextran Sulphate-Sodium salt colitis model

C57BL/6 wild-type mice were maintained under pathogen-free conditions and housed in filter-top cages at the animal facility of Fondazione IRCCS Istituto Nazionale dei Tumori, Milano. Animal experiments were approved by the Institutional Ethics Committee for Animal Experimentation and by the Italian Ministry of Health (Authorization Number INT07/2009).

DSS (ThermoFisher Scientific, Italy) was administered for 10 days in drinking water at 1.5% w/v. Monitoring loss of body weight from day 0 was used to follow disease course. After DSS withdrawal, mice were followed for transition from acute inflammation to the recovery phase.

Histology

Colons were dissected without exposure to DSS or after 3, 10, 14 and 17 days, washed in phosphate-buffered saline (PBS), fixed and embedding in paraffin wax. The extent of colon inflammation was determined by analysing grade and extension of colitis and glandular dysplasia.[21,22]

Human tissues

Use of human material received ethical approval (P/01/023) and all participants provided written informed consent. Samples from human sporadic rectal cancer, active and inactive CD and tumour from ulcerative colitis (UC) patient were used for both immunohistochemistry (IHC) and ISH studies. Intramucosal glands within airways were used as positive control tissues only.

In Situ Hybridisation

Probe sets for specific detection of mouse *Duox2*, *Duoxa2* and *Lpo* and human *DUOX2* and *LPO mRNAs*, together with appropriate positive control (peptidylprolyl isomerase B, *PPIB* and *Ppib*) and negative control (dihydrodipicolinate reductase, *Dapb*) probe sets and RNAscope® 2.0 (brown) kits were purchased from Advanced Cell Diagnostics (ACD) (Newark, CA, USA). These were used on 4 µm sections following manufacturer's instructions (protease treatment at 1:15, incubations at 40 °C in HybEz oven). Dual ISH for *Duox2* and *Duoxa2* yielding green/blue and red signals respectively was carried out as a contract service by ACD: serial sections were hybridised with either *Duox2* probe, *Duoxa2* probe, both probes, or no probe to allow colocalisation and any non-specific signals to be assessed in mouse tissues from d0, d3 and d10 of DSS protocol. Slides were scanned using a 20x objective (NanoZoomer 2.0 H-T, Hamamatsu Photonics UK Limited, Welwyn Garden City, UK) and saved as .ndpi files. For mouse sections NDPview2 for Macintosh (Hamamatsu Photonics UK Limited) was used to make .ndpa annotations marking areas showing well-orientated crypts of normal appearance, close to mucosa inflammation, or of regenerative phenotype (poorly differentiated epithelium, mitoses other than close to crypt bases, goblet cell depletion) that were viewed with a x60 virtual objective then exported as .tiff files (Fig., Supplemental Digital Content 1 for examples). Adobe Photoshop CS5 (www.adobe.com/uk/) and a Wacom Bamboo graphics tablet (www.wacom.eu) were used to mark manually (with a 9 pixel tool) the position of each of up to several hundred mRNA signal dots per crypt in multiple individual crypts for each probe at each timepoint. A scalar element marked quintiles and the polygonal lasso tool estimated by area the number of signal pixels in each fifth of each crypt assessed. Crypt height was assessed by comparison with the scale bar from NDPview2 (Fig., Supplemental Digital

Content 1).

Reverse Transcription- quantitative PCR (RT-qPCR) analysis

Colons were rinsed with PBS, homogenized in Trizol reagent and total RNA extracted using RNAeasy Mini Kits (Qiagen, Tokyo, Japan), quantified and checked for purity by spectrophotometry (Nanodrop, Thermo Scientific). RNA (100ng) was reverse transcribed using a High Capacity cDNA Reverse Transcription Kit (Applied Biosystems). The qPCR steps used *Duox2*, *Lpo* and *Rplpo* (large ribosomal protein RNA; internal control) probe sets (Life Technologies) with n=40 amplification cycles according to the manufacturer's protocol. Melt curve analysis supported that only single products accumulated. Relative fold-change normalised to *Rplpo* was calculated for each mouse.

Statistical analyses

Statistical analysis was performed in R statistical programming language using the (non)linear mixed effects model package (nlme). Nested linear mixed effects models tested various hypotheses (see Results section) adjusting for possible confounding factors such as mouse-specific or crypt-specific effects. Nested models imposed increasing levels of model complexity (interactions) and the most significant models were chosen by comparing the likelihoods associated with the different models using the anova() function.

cDNA microarray analysis

To investigate *LPO* expression levels in human large intestine we interrogated the GEO database and extracted three studies that have generated gene expression profiles of multiple normal human tissues. Study A measured whole genome expression in 31

human tissues using an ABI human genome array.[23] Study B generated gene expression profiles of 42 normal human tissues on custom high-density microarrays.[24] Study C performed genome-wide expression profiling of 36 types of normal human tissues using an Affymetrix Human Genome Array.[25] We extracted the GEO profile graphs of the probes that correspond to *LPO* gene and summarised the expression values for normal tissue of interest (colon) and tissues for which expression of *LPO* is highest (salivary gland and trachea).

To further investigate *LPO* expression levels in human large intestine during inflammation and in comparison to *DUOX2* we extracted three additional studies on UC. Study A performed whole-genome transcriptional analysis of colonic biopsies from patients with histologically active (n=15) and inactive UC (n=7), and non-IBD controls (n=13) using an Affymetrix microarray.[26] Study B analysed inflamed (n=63) and un-inflamed (n=66) colon epithelial biopsies of 67 UC patients from different anatomical locations of the gastrointestinal tract using an Agilent microarray platform.[27] Finally, study C analysed colonic mucosa samples from UC patients with (n=8) or without (n=13) signs of inflammation using an Affymetrix microarray.[28] We again extracted GEO profile graphs of probes that correspond to *LPO* and *DUOX2* genes and summarised expression values across replicates. To test for statistically significant differences between conditions, two-sided Student's *t*-test was used. It should be noted that since each study has used a different microarray platform and normalisation method, the expression levels presented are not always on the same scale and hence we cannot directly perform a between-studies comparison.

RESULTS

Distribution of *Duox2* and *Lpo* mRNAs is different in normal colonic crypts

Analysis of homogenates although quantitative, or relative to an internal control such as a ribosomal protein RNA, cannot reveal which cells are expressing the mRNAs or where changes occur during the acute and recovery phases of DSS colitis. We assessed this by ISH using RNAscope 2.0 branched DNA detection. We chose this ISH technology because of its intrinsic high specificity and sensitivity that results in a brown dot of reaction product potentially from each single mRNA (see Fig., Supplemental Digital Content 1). We confined our transcript counting to crypts in regions that presented good longitudinal sections that gave results for all probes, and this precluded scoring tortuous crypts or assessing incomplete regenerative monolayers. The distributions of *Duox2* and *Lpo* mRNAs in normal crypts prior to DSS exposure were clearly different: both were expressed exclusively in epithelial cells, but *Duox2* was expressed mostly in the upper quintile close to the gut lumen and potential pathogens, whereas most *Lpo* was found in the basal quintile, where proliferative and stem cells reside (Fig. 1).

Distribution of *Duox2* mRNA expression alters during the acute colitic phases and regeneration

To assess whether and how *Duox2* and *Lpo* expression were modulated in a condition of inflammation, C57BL/6 animals were treated with DSS to induce colitis. Mice developed symptoms and showed intestinal pathology as expected from the dose of DSS and the susceptibility of the C57BL/6 strain used (Fig. 2A, B). In the initial acute phase (d3), *Duox2* remained abundant at the tops of crypts but also became expressed strongly in crypt bases; this disturbance resolved in crypts of normal appearance over the next week. Crypts near inflammation showed disturbed patterns of expression in the acute phase that became more normal in the recovery phase. Crypts adjacent to ulceration and of regenerative phenotype were recognised at d10, d14 and d17, and

these elongated glands initially showed no gradient of *Duox2* expression (Fig. 3A), but these matured somewhat to reflect the patterns seen in inflamed crypts (Fig. 3B).

We assessed our observation statistically using three nested linear models with (i) no day effect, (ii) fixed day effect and a (iii) quintile-day interaction effect. The quintile-day interaction model was found to be the best model suggesting that the distribution of *Duox2* mRNA does indeed change during the time course. Examining regression coefficients, the coefficients associated with quintile C on d3 ($p = 0.0002$) and quintile B and C on d10 ($p = 0.0026$ and $p = 0.0022$) were significant and showed a reduction in *Duox2*. Next, we tested whether distribution of *Duox2* within normal and inflamed crypts alters on each of the five days using linear models with and without normal-inflammation interaction terms. The model including the normal-inflammation interaction term was statistically significant on days 0, 10 and 14 ($p < 0.001$, $p < 0.001$ and $p=0.0015$, respectively) indicating differences in distributions in inflamed crypts compared to normal crypts. We then asked whether the distribution of *Duox2* in regenerative crypts was similar to the normal or inflamed pattern, and does this change through the time course? This involved comparing the distribution between normal, inflamed and regenerative crypts on all days for which data was available. In all instances, there was a statistically significant difference between the regenerative crypts and normal/inflamed crypts on the same day ($p < 0.0001$). The distribution of *Duox2* also changed in regenerative crypts over time (day 14-17; Fig. 3A).

Distribution of *Lpo* and *Duox2* is different in normal, inflamed and regenerative crypts

Distribution and time-course changes were then examined for *Lpo* expression (Fig. 3C, D). Again, we compared three nested linear models with (i) no day effect, (ii) fixed day

effect and a (iii) quintile-day interaction effect. The quintile-day interaction model was found to be the best model suggesting that the distribution of *Lpo* mRNA does indeed change during the time course, with the most basal quintile E (containing the stem cell compartment) on d10 and the second most-basal quintile D (containing transit amplifying cells) on d14 showing distinct differences. When the differences in the distribution of *Lpo* between normal and inflamed crypts on each of the five days were examined, all days showed ($p < 0.001$) statistically significant differences in *Lpo* distributions in inflamed crypts compared to normal crypts.

Lpo was detected in regenerative monolayer epithelium and deep in branching regenerative epithelial structures (Fig., Supplemental Digital Content 2), whereas *Duox2* was expressed most strongly in surface compartments. Maintaining expression of Lpo in crypt bases for production of hypothiocyanate would be predicted to help consume H_2O_2 that had diffused to these important regions. Crypts adjacent to ulceration and of regenerative phenotype were recognised at d10, d14 and d17, and these elongated glands initially showed no gradient of *Duox2* expression yet had basally-polarized *Lpo* expression, (Fig. 3C). Over the time course these patterns matured somewhat towards those of inflamed crypts. When regenerative and normal crypts were compared, we found only significantly differences in distribution of *Lpo* on d10 and d14. In comparison with inflamed crypts, significant differences in distribution of *Lpo* were only found on d10 and d17 ($p = 0.0223$ and $p = 0.0294$, respectively). The pattern of expression of *Lpo* differed from that of *Duox2* in normal or inflamed or regenerative crypts in all instances ($p < 0.001$).

Next, we used the RT-qPCR assessment of mRNA expression in homogenates to obtain a broad idea of the change in the ratios of the *Duox2*, *Duoxa2* and *Lpo*

transcripts. *Duox2,* but not *Lpo* levels were increased during the acute phase of response to DSS. *Duox2* increased at d3 and d11 during the acute phase, and was still increased at d14, falling to normal levels or below at d17; *Duoxa2* followed the same approximate pattern (see Fig. A, B, Supplemental Digital Content 3). In contrast, expression of *Lpo* followed a different pattern dipping slightly at d3 then increasing to a maximum at d14 (see Supplemental Digital Content 3, C). As *Duox2*, *Duoxa2* and *Lpo* expression were confined to epithelial cell types there would be no benefit in separating the epithelium from stromal cell types (or cells derived from haematopoietic lineages) for RT-qPCR experiments. Importantly, the ISH allowed us to look at the distributions and ratios of mRNAs along the crypt axis.

Expression of *Duox2* and *Duoxa2* is regulated independently

As the gene encoding Duox2 and the gene encoding its obligate accessory protein Duoxa2 are adjacent in a head-to-head arrangement, we asked whether *Duox2* expression was co-ordinated with that of *Duoxa2* in the acute phase of DSS colitis. We quantified these separately in near serial sections, and also examined sections with both mRNAs detected together in different colours. *Duoxa2* mRNA had a more extreme apically-focussed pattern of expression than did *Duox2* (Fig. 4A, B). This supports the contention that H_2O_2 production would normally be confined to the luminal surface, closest to gut pathogens and remote from the stem cell compartment where DNA damage might have long-lasting consequences. After initiation of DSS colitis, at d3 and d10 normal crypts and crypts near inflammation showed much more extensive zones in which both *Duoxa2* and *Duox2* were abundant, and potentially H_2O_2 production would be enhanced (Fig. 4C).

Absence of expression of human lactoperoxidase in the human intestine.

Using ISH we and others have been able to detect *DUOX2* mRNA expression in intestinal epithelium of patients with UC (reported previously in [3]) and in Figure 5 we show detection of *DUOX2* in normal surface epithelium and a cancer from a UC patient (Fig. 5A-D) whilst *LPO* was not detected in serial sections (Fig. 5E-H). In addition, using ISH we found *DUOX2*, but not *LPO* mRNA, detectable in the small intestine of a Crohn's Disease patient. We established that the LPO ISH probeset worked (positive control) by detecting *LPO* expression in human upper airway glandular epithelium (see Supplemental Digital Content 4).

We sought further confirmation of our ISH findings by interrogating the gene signatures from cDNA microarray analysis of multiple normal tissues performed by three independent studies (Study A-C).[23-25] Our analysis found that *LPO* is not expressed in most human tissues including colon (see Supplemental Digital Content 5), but shows high levels of expression in salivary gland and trachea (Fig. 6A). To confirm the absence of expression of human *LPO* during inflammation, we interrogated the expression profiles of *LPO* in UC as measured by three independent studies, Study A-C.[26-28] We found that although *DUOX2* expression in colon increases during inflammation (two-sided *t*-test p-value between UC inflamed and controls: 3.933×10^{-08}, 1.435×10^{-13} and 0.0001147 for each of three studies respectively), *LPO* remains unchanged (two-sided t-test p-value between UC inflamed and controls: 0.1043, 0.06567 and 0.6089 for each of three studies respectively) (Figure 6B and see Supplemental Digital Content 6).

DISCUSSION

Previous studies attempted to localize DUOX2 in non-DSS exposed human and rodent gut tissue and organoids, but were limited by issues with methodology.[29-32] For

example, El Hassani and colleagues showed evidence for localization of human DUOX2 by using a rabbit polyclonal antiserum, but that also stained the muscularis mucosae non-specifically.[29] Apical immunofluorescence for Duox was shown in mouse cells grown as organoids, but this relied on a pan-duox antibody.[30] ISH using a ^{35}S riboprobe was interpreted to show that *duox2* mRNA was present predominantly in the lower half of rat rectal crypts,[31] but this gross distribution conflicts with more recent data from analysis of mRNA from laser capture microdissection of mouse mucosa in which apical colonic 'tip' pooled RNA had higher levels of *Duox2* mRNA than 'crypt base + lamina propria'.[32] No previous study has localised *Duox2*, *Duoxa2* and *Lpo* or studied the effects of DSS.

We found in the mouse that *Duox2* and *Duoxa2* are expressed in crypts of the large bowel normally in a gradient with the strongest expression at the luminal aspect of crypts. In crypts close to inflammation the distribution of these mRNAs is perturbed – spreading more broadly throughout the crypt. In human UC we reported accentuation of *DUOX2* and *DUOXA2* expression in crypt abscesses that are a feature of human UC, but unusual in the mouse (Supplemental Digital Content 2).[3] In mouse, we found that the normal patterns of *Duox2*/*Duoxa2 and Lpo* expression were disrupted following DSS exposure; the wider availability of these proteins along the crypt would permit generation of greater H_2O_2 concentrations nearer the crypt base and with the potential for genetic damage in stem cells. Such damage might explain partly the increased risk of CRC in IBD patients.[33]

The DSS colitis protocol limits sampling to discrete time points: here, we made observations by ISH and counted transcripts at Day 0 (no DSS treatment) and at Day 3 and Day 10 during the acute phase and Day 14 and Day 17 during the recovery phase.

In the absence of continuous monitoring, only a limited number of snapshots of the progressive changes in expression can be provided. Nevertheless, we can provide the first assessment of *Duox2/Duoxa2* changes in the mouse DSS-induced colitic colon. We have found that the two obligate genes for direct production of H_2O_2 are affected in broadly similar ways during the induction and resolution of DSS colitis in mice. However, *Duoxa2* appears more tightly confined and may be subject to subtly different regulation potentially to limit any genetic damage to stem cells at the base of crypts. Studies of isolated crypts would offer a way to resolve more precisely the rapidity of each genes' response to DSS, other damaging agents or bacteria and the potential to assess the site of production and yield of H_2O_2 using very specific probes recently developed.[30 34] To our knowledge there are at present no specific inhibitors of Duox2/Duoxa2 or Lpo with which to study the action of this system *ex vivo*, so it may be necessary to pursue knockdown strategies to determine the protective effects of Lpo against DNA damage in isolated murine crypts. However, if LPO is absent from human crypts, mouse models of colitis for understanding the risk of cancer in colitis will not take into account this difference between species.

LPO is important for generating biocidal compounds for bacterial defence following breaches in epithelial integrity and for consuming the additional H_2O_2 produced in response to damage that might otherwise damage host cell DNA. Lpo expression in the mouse gut has been assessed immunohistochemically and at the mRNA level, and varies between mouse strains.[20] By immunohistochemistry, Lpo appears apical [20], yet data within supplementary tables of Sommer et al support *Lpo* being basal in dissected normal crypts (± germ free),[35] and our present results show it is normally basal, but more widespread in regenerative gland epithelium. In distinct contrast to the mouse, we were surprised to find little or no support for expression of *LPO* in the human large

bowel. In contrast, LPO protein and mRNA are expressed in human intramucosal glands of high order airways. The human *LPO* probe we used gave clear signals in positive control airway tissue, but not in the large bowel. Similarly, IHC could detect no protein expression and we did not find evidence for *LPO* expression in human large bowel samples during analysis of available microarray data sets for UC and normal bowel tissues. These findings support our experimental evidence that LPO is largely absent in human large bowel. We perceive this deficit to be a major unexplained difference in host defence between man and mouse.

In conclusion, H_2O_2 is needed to help in the recruitment of immune cells, mucosal healing and the resolution of inflammation. The presence of LPO together with H_2O_2 could assist defence via the production of OSCN-. We propose that in mice there is a spatial separation of the products of the *Lpo* and the *Duox2/Duoxa2* genes. Normally the *Duox2/Duoxa2* genes place the greatest production of H_2O_2 towards the lumen of the intestine and basal expression of Lpo confines H_2O_2 scavenging and the production of the biocidal OSCN- to the crypt base as a second line defense against certain pathogens reaching the crypt base. This arrangement would serve to reduce the likelihood of enduring DNA damage. Moreover, the increased levels of *Lpo* during the recovery phase from colitis in mice might support both scavenging and OSCN- production in vulnerable epithelium. Mice and men may have evolved different mechanisms to cope with their common gut pathogens, although both mechanisms serve to maintain H_2O_2 as a means of enhancing mucosal healing by limiting the extent of scavenging. However, the lack of an *LPO* scavenging action in human gut might increase susceptibility to DNA damage including rearrangements unless other mechanisms exist.

ACKNOWLEDGEMENTS

The authors are grateful to Li-Chong Wang (Advanced Cell Diagnostics) for conducting the service dual ISH, and the Core Pathology Service, Blizard Institute, for cutting FFPE sections. We also thank Sam Janes for facilitating access to positive control tissues. RP was funded by the Monument Trust. MPC was funded by the CARIPLO Foundation (project 2010-0790) and the Italian Ministry of Health. AR was supported by an annual fellowship from Fondazione Umberto Veronesi.

AUTHOR CONTRIBUTIONS (if needed by journal)

AR, RP, RJ, SM conducted experiments; AL, CY, EG performed bioinformatics and data analysis, RF reviewed histopathology; JOL, MP, AS conceived the project and obtained funding; all authors contributed to drafting and subsequent revisions of the manuscript, and approved the final manuscript.

REFERENCES

1. Bae YS, Choi MK, Lee WJ. Dual oxidase in mucosal immunity and host-microbe homeostasis. *Trends Immunol.* 2010;31:278–287.

2. Bedard K, Krause KH. The NOX family of ROS-generating NADPH oxidases: physiology and pathophysiology. *Physiol Rev.* 2007;87:245–313.

3. MacFie TS, Poulsom R, Parker A, et al. DUOX2 and DUOXA2 form the predominant

enzyme system capable of producing the reactive oxygen species H_2O_2 in active ulcerative colitis and are modulated by 5-aminosalicylic acid. *Inflamm Bowel Dis.* 2014;20:514-524.

4. Grasberger H, Mohamad El-Zaatari M, Juanita L, et al. Dual oxidases control release of hydrogen peroxide by the gastric epithelium to prevent *Helicobacter felis* infection and inflammation in mice. *Gastroenterology.* 2013;145:1045–1054.

5. Atack JM, Kelly DJ. Oxidative stress in *Campylobacter jejuni*: responses, resistance and regulation. *Future Microbiol.* 2009;4:677–900.

6. Mori M, Suzuki H, Suzuki M, et al. Catalase and superoxide dismutase secreted from *Helicobacter pylori*. *Helicobacter.* 1997;2:100–105.

7. Fox JG, Dewhirst FE, Tully JG, et al. *Helicobacter hepaticus sp nov*, a microaerophilic bacterium isolated from livers and intestinal mucosal scrapings from mice. *J Clin Microbiol.* 1994;32:1238–1245.

8. Taylor WI, Achanzar D. Catalase test as an aid to the identification of *Enterobacteriaceae*. Appl *Microbiol.* 1972;24:58–61.

9. Chang D, Hu ZL, Zhang L, et al. Association of catalase genotype with oxidative stress in the predication of colorectal cancer: modification by epidemiological factors. *Biomed Environ Sci.* 2012;25:156–162.

10. Monari M, Foschi J, Calabrese C, et al. Implications of antioxidant enzymes in

human gastric neoplasms. *Int J Mol Med.* 2009;24:693–700.

11. Iborra M, Moret I, Rausell F, et al. Role of oxidative stress and antioxidant enzymes in Crohn's disease. *Biochem Soc Trans.* 2011; **39**: 1102–1106.

12. De Moreno de LA, LeBlanc JG, Perdigon G, et al. Oral administration of a catalase-producing *Lactococcus lactis* can prevent a chemically induced colon cancer in mice. *J Med Microbiol.* 2008;57:100–105.

13. LeBlanc JG, del CS, Miyoshi A, et al. Use of superoxide dismutase and catalase producing lactic acid bacteria in TNBS induced Crohn's disease in mice. *J Biotechnol.* 2011;151:287–293.

14. Lee KA, Kim SH, Kim EK, et al. Bacterial-derived uracil as a modulator of mucosal immunity and gut-microbe homeostasis in Drosophila. *Cell.* 2013;153:797–811.

15. Modi S, Deodhar SS, Behere DV, et al. Lactoperoxidase-catalyzed oxidation of thiocyanate by hydrogen peroxide: 15N nuclear magnetic resonance and optical spectral studies. *Biochemistry.* 1991;30:118-124.

16. D'Errico M, Parlanti E, Dogliotti E. Mechanism of oxidative DNA damage repair and relevance to human pathology. *Mutat Res*. 2008;659:4–14.

17. Xu Y, Szep S, Lu Z. The antioxidant role of thiocyanate in the pathogenesis of cystic fibrosis and other inflammation-related diseases. *Proc Natl Acad Sci USA.* 2009;106:20515–20519.

18. Esworthy RS, Aranda R, Martin MG, et al. Mice with combined disruption of Gpx1 and Gpx2 genes have colitis. *Am J Physiol Gastrointest Liver Physiol.* 2001;281:G848–G855.

19. Esworthy RS, Kim B-W, Rivas GE, et al. Analysis of candidate colitis genes in the Gdac1 locus of mice deficient in glutathione peroxidase-1 and -2. *PLoS ONE.* 2012;7:e44262.

20. Kim B-W, R. Esworthy RS, Hahn MA, et al. Expression of lactoperoxidase in differentiated mouse colon epithelial cells. *Free Radical Biol Med.* 2012;52:1569-1576.

21. Egger B, Procaccino F, Lakshmanan J, et al. Mice lacking transforming growth factor alpha have an increased susceptibility to dextran sulfate-induced colitis. *Gastroenterology.* 1997;113:825-832.

22. Rigoni A, Bongiovanni L, Burocchi A, et al. Mast Cells Infiltrating Inflamed or Transformed Gut Alternatively Sustain Mucosal Healing or Tumor Growth. *Cancer Res.* 2015;75:3760-3770.

23. Dezso Z, Nikolsky Y, Sviridov E, et al. A comprehensive functional analysis of tissue specificity of human gene expression. *BMC Biol.* 2008;6:49.

24. She X, Rohl CA, Castle JC, et al. Definition, conservation and epigenetics of housekeeping and tissue-enriched genes. *BMC Genomics.* 2009;10:269.

25. Ge X, Yamamoto S, Tsutsumi S, *et al*. Interpreting expression profiles of cancers by genome-wide survey of breadth of expression in normal tissues. *Genomics.* 2005;86:127-141.

26. Planell N, Lozano JJ, Mora-Buch R, *et al*. Transcriptional analysis of the intestinal mucosa of patients with ulcerative colitis in remission reveals lasting epithelial cell alterations. *Gut.* 2013;62:967-976.

27. Noble CL, Abbas AR, Cornelius J, *et al*. Regional variation in gene expression in the healthy colon is dysregulated in ulcerative colitis. *Gut.* 2008;57:1398-1405.

28. Olsen J, Gerds TA, Seidelin JB, *et al*. Diagnosis of ulcerative colitis before onset of inflammation by multivariate modeling of genome-wide gene expression data. *Inflamm Bowel Dis.* 2009;15:1032-1038.

29. El Hassani RA, Benfares N, Caillou B, et al. Dual oxidase2 is expressed all along the digestive tract. *Am J Physiol Gastrointest Liver Physiol*. 2005;288:G933-42.

30. Grasberger H, Gao J, Nagao-Kitamoto H, et al. Increased expression of DUOX2 is an epithelial response to mucosal dysbiosis required for immune homeostasis in mouse intestine. *Gastroenterology*. 2015;149:1849-59.

31. Geiszt M, Witta J, Baffi J, et al. Dual oxidases represent novel hydrogen peroxide sources supporting mucosal surface host defense. FASEB J. 2003;17:1502-1504.

32. Sommer F, Bäckhed F. The gut microbiota engages different signaling pathways to

induce Duox2 expression in the ileum and colon epithelium. *Mucosal Immunol*. 2015;8:372-379.

33. Jess T, Rungoe C, Peyrin-Biroulet L. Risk of colorectal cancer in patients with ulcerative colitis: a meta-analysis of population-based cohort studies. *Clin Gastroenterol Hepatol.* 2012;10:639-645.

34. Daniel KB, Agrawal A, Manchester M, et al. Readily accessible Fluorescent Probes for Sensitive Biological Imaging of Hydrogen Peroxide. *Chembiochem.* 2013;14:593–598.

35. Sommer F, Nookaew I, Sommer N, et al. Site-specific programming of the host epithelial transcriptome by the gut microbiota. Genome Biol. 2015;16(1):62.

FIGURE LEGENDS

Figure 1. **Crypt height and the distribution of *Duox2* and *Lpo* within crypts of normal appearance before and after exposure to dextran sodium sulphate.** (A) *Duox2* and (B) *Lpo* expression in normal crypts at the different time point. Pale blue cross shows mean and standard error of mean of crypt height. n= indicates the numbers of crypts assessed for signals with the indicated probe.

Figure 2. **Experimental protocol, body weight and intestinal changes in response to dextran sodium sulphate.** (A) Experimental protocol. Time points are given as days. Numbers of mice studied overall and number studied using ISH are shown. Dextran Sodium Sulphate, DSS. (B) H&E of colon rolls at 0, 3, 10, 14, 17 days. Scale

bar is 1 mm. The area indicated by an arrow is shown below (scale bar is 250 μm) At 0 days crypts were of normal morphology. At day 3 (acute phase) just one focus in this colon at this level showed mucosal injury induced by DSS. At day 10 (end of DSS exposure), damage was more extensive; this region shows inflammatory cells within the mucosa and submucosa, several crypts with limited goblet cell morphology and abscess-like dilatation; the surface epithelium appears intact. At day 14 (recovery phase), extensive ulceration and areas with regenerative glandular structures are evident; this region has an almost continuous epithelial covering flanked by simple regenerative crypts. At day 17, ulcerated mucosa and regenerating patches are still present, but large areas of mucosa appear macroscopically normal; this region shows branching/budding crypt bases surrounded by inflamed stroma, similar to the structures expressing *Lpo* basally in Supplemental Digital Content 2.

Figure 3. ***Duox2*** **and** ***Lpo*** **expression in crypts near inflammation and in regenerative crypts after dextran sodium sulphate exposure in mice.** (A) *Duox2* expression in crypts at the different time point. (B*)* Representative images of *Duox2 in situ* hybridisation at day 10 and 14. (C) *Lpo* expression in crypts at the different time point. (D*)* Representative images of *Lpo in situ* hybridisation at day 10 and 14. n= indicates the numbers of crypts assessed for signals with the indicated probe. Pale blue cross shows mean and standard error of mean of crypt height. See Supplemental Digital Content 2 for additional examples.

Figure 4. **Effects of dextran sodium sulphate on the distribution of** ***Duoxa2***, ***Duox2*** **and the ratio** ***Duoxa2:Duox2*** **within crypts.** Crypt height is given by reference to scale bar. The *Duoxa2:Duox2* ratio used average values for each quintile. Pale blue cross shows mean and standard error of mean of crypt height.

Figure 5. **The presence of *DUOX2* and absence of *LPO* in intestinal epithelium and cancer from a patient with ulcerative colitis (UC).** (A) ISH for *DUOX2* in normal epithelium from an UC patient shown at low power; (B) ISH for *LPO* in normal epithelium of the same UC patient at low power; (C) *DUOX2* in normal epithelium from UC patient shown at high power**.** (D) *LPO* in normal epithelium from UC patient at high power**.** (E) *DUOX2* in cancer from UC patient at low power**.** (F) *LPO* in cancer from UC patient at low power. (G) *DUOX2* in cancer from UC patient at high power**.** (H) *LPO* in cancer from UC patient at high power. Arrows denote positive cells. Low power scale bars = 250 μm, high power scale bars = 50 μm. See also Supplemental Digital Content 4.

Figure 6. ***LPO* is expressed at high levels in salivary gland and trachea and is unresponsive to inflammation in the ulcerative colitis colon.** (A) *LPO* expression in salivary gland, trachea and colon as measured by three microarray studies (Study A-C).[23-25] (B) LPO and DUOX2 expression in UC inflamed colon, UC uninflamed colon and controls as measured by three additional microarray studies (Study A: colonic biopsies from patients with histologically active (n=15) and inactive UC (n=7), and non-IBD controls (n=13);[26] Study B: inflamed (n=63) and un-inflamed (n=66) colon epithelial biopsies of 67 UC patients;[27] and Study C: colonic mucosa samples from UC patients with (n=8) or without (n=13) signs of inflammation).[28]

SUPPLEMENTAL DIGITAL CONTENTS

Supplemental figure legends

Supplemental digital content 1. **Examples of *Duox2*, *Duoxa2* and *Lpo* mRNA ISH signal dots and their counting in quintiles.** (A) An example of an image exported from a NanoZoomer scan, with *Duox2* mRNA signal brown dots (in a region of D17 mouse colon with crypts of normal appearance) marked in magenta with a 9 pixel brush and with quintile scale in place. Total signal area (pixels) was measured for each fifth of an individual crypt's height. Crypt height was scaled from the size bar generated in NDPview2 software. (B) An example of *Duoxa2* mRNA signals (marked when scored) in normal crypts of a D0 mouse colon; not that signals are tightly grouped in the most apical fifth of the crypt. (C) A pair of near-serial sections showing *Duox2* (left) and *Lpo* (right) mRNA ISH signals in a large crowded crypt with limited goblet cell phenotypes and considered regenerative in the colon of a D14 mouse. Note that nearby inflammatory cells show no ISH signals.

Supplemental digital content 2. **Examples of ISH results showing *Duox2*, *Duoxa2* or *Lpo* expression patterns in features of DSS colitis.** D10, both *Duox2* (blue/green signal dots) and *Duoxa2* mRNAs (red signal dots; near–serial section) are abundant apically, but also deep within regenerating glands (RG) in this severely inflamed region of colon. No expression was detected outside the epithelium. Note that individual ISH signal dots are smaller than one pixel in these panels. D14, widespread expression of *Duoxa2* and *Lpo* mRNAs deep within crypts; *Duox2* is conspicuous in the abscessed crypts (*) in this inflamed area. D14 lower row, the intact epithelial monolayer (m) of a

healing ulcer expresses *Duox2* and variably *Lpo* mRNAs; the orientation is not perfectly in cross-section, but mRNA signals appear located mainly towards the apical surface of the epithelial monolayer. D17, *Duox2* and to a much lesser extent *Lpo* mRNAs are present in the epithelial monolayer (m) in this late-stage lesion. The lymphoid aggregates (LA) and other stromal components appear unlabelled, yet both mRNAs are present throughout the epithelium, with *Lpo* conspicuously abundant deep in the branching/bifurcating glands. Individual signal dots can be seen in the enlarged regions indicated by red and green boxes.

Supplemental digital content 3. ***Duox2,* but not *Lpo* abundance increases during the acute phase of response to DSS in the drinking water of mice.** Relative levels of *Duox2* mRNA (panel A)*, Duoxa2* (B) *and Lpo* (C) *assessed by* RT-qPCR. Number of mice shown on bars. Statistical differences were evaluated using one-way ANOVA corrected for multiple testing and no significant differences were identified between day 0 and days post-exposure for A-C.

Supplemental digital content 4. ***LPO* is expressed in human upper airway but not in the intestine of Crohn's disease patients with active disease.** (A) *DUOX2* expression is present in Crohn's Disease small bowel with active disease: areas 1 and 2 shown at greater magnification below. (B) *LPO* expression is not detectable in a section serial to A: areas 1 and 2 shown at greater magnification below. (C) *LPO* expression is detected in human upper airway glandular epithelium used as a positive-tissue control: areas 1 and 2 shown at greater magnification below. Low power scale bars = 250 μm, high power scale bars = 50 μm.

Supplemental digital content 5. ***LPO* is not expressed in the colon or most other human tissues.** GEO profile graphs of the probes that correspond to the *LPO* gene as quantified by three microarray studies (Study A-C).[23-25]

Supplemental digital content 6. **Data for *DUOX2* and *LPO* in the inflamed colon of ulcerative colitis patients.** GEO profile graphs of the probes that correspond to *LPO* and *DUOX2* genes as quantified by three microarray studies (Study A-C).[26-28]

Figure 1

Click here to download Image Figure 1.tif

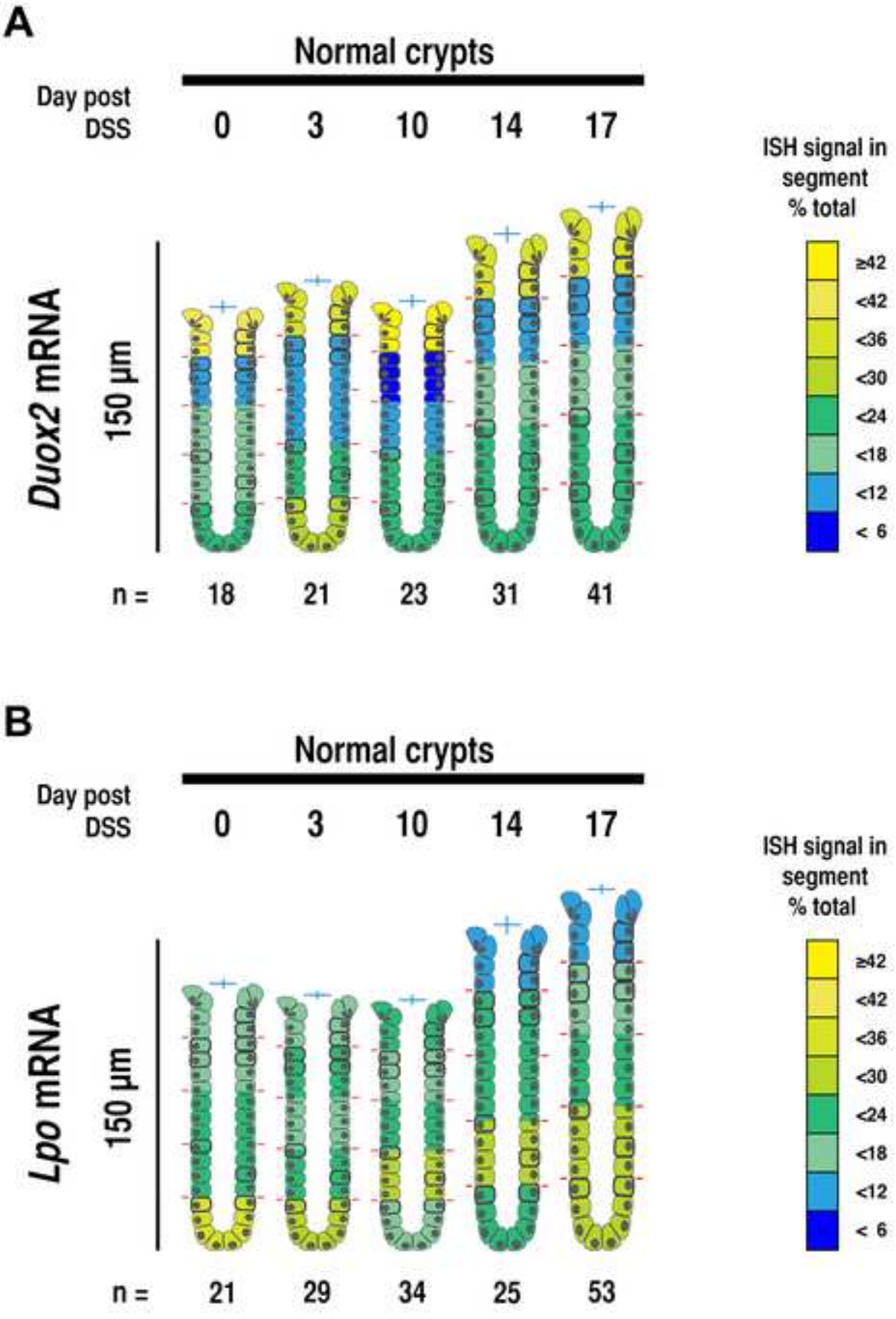

Figure 2

Click here to download Image Figure 2.tif

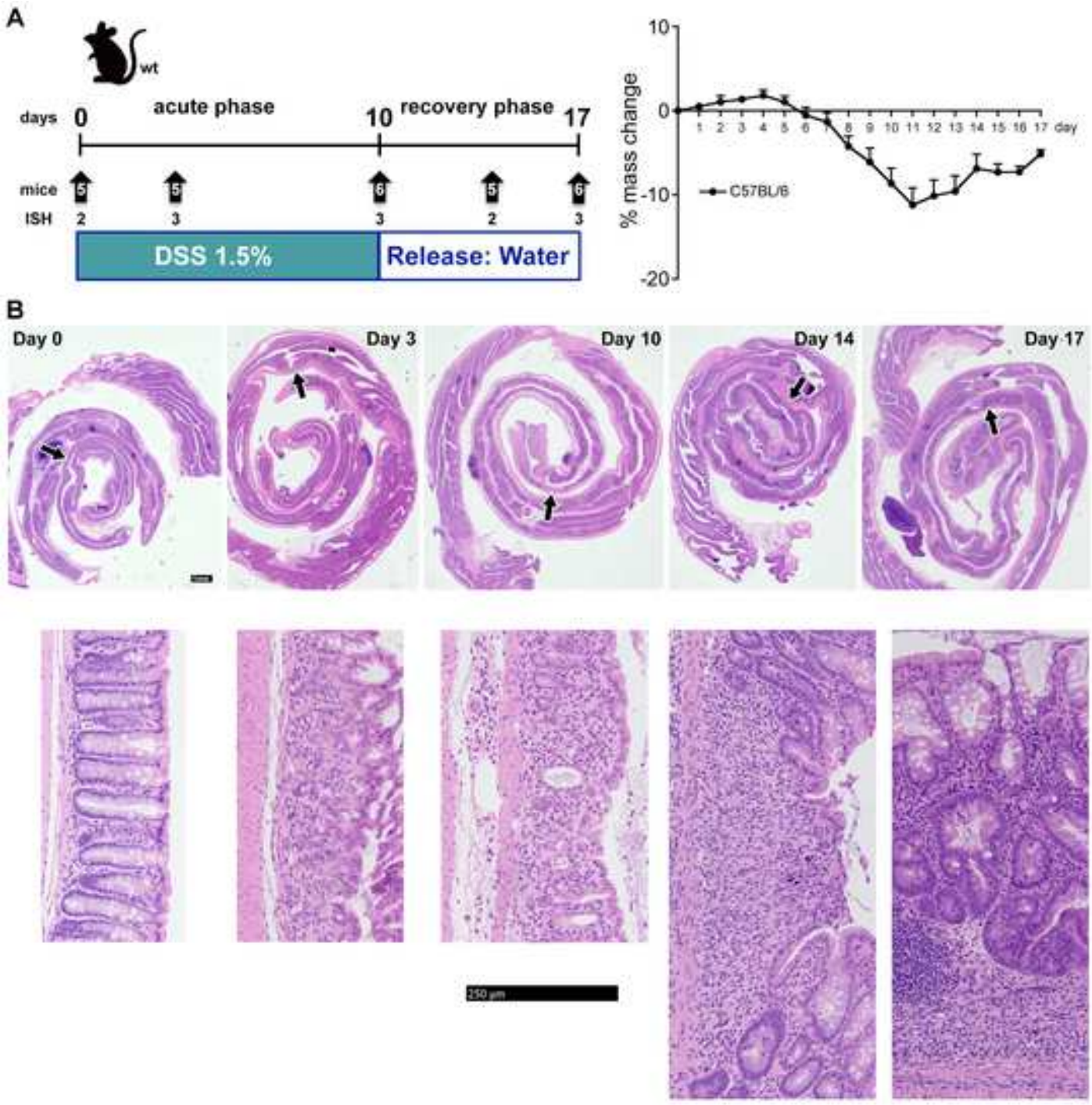

Figure 3

Click here to download Image Figure 3.tif

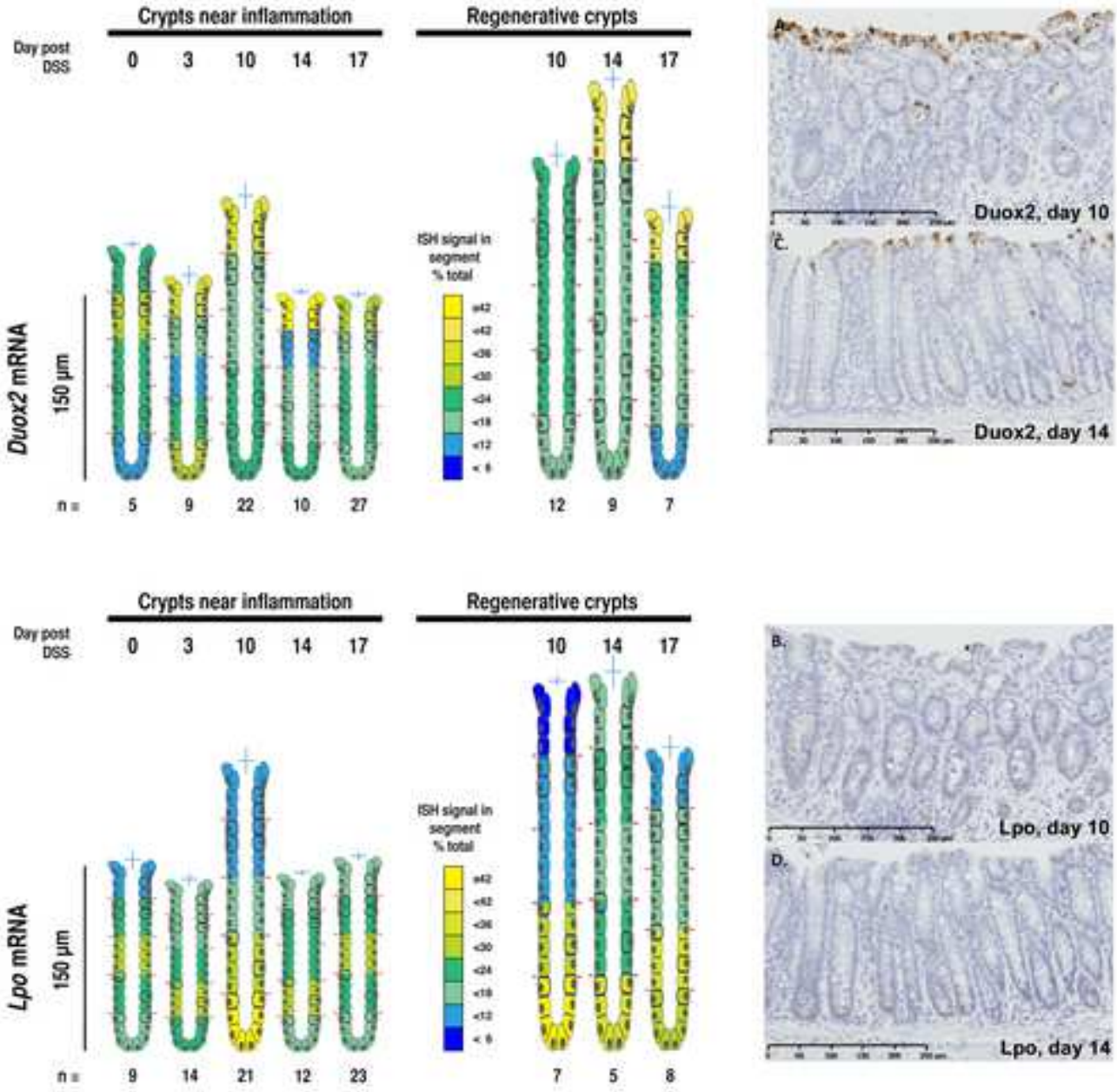

Figure 4

Click here to download Image Figure 4.tif

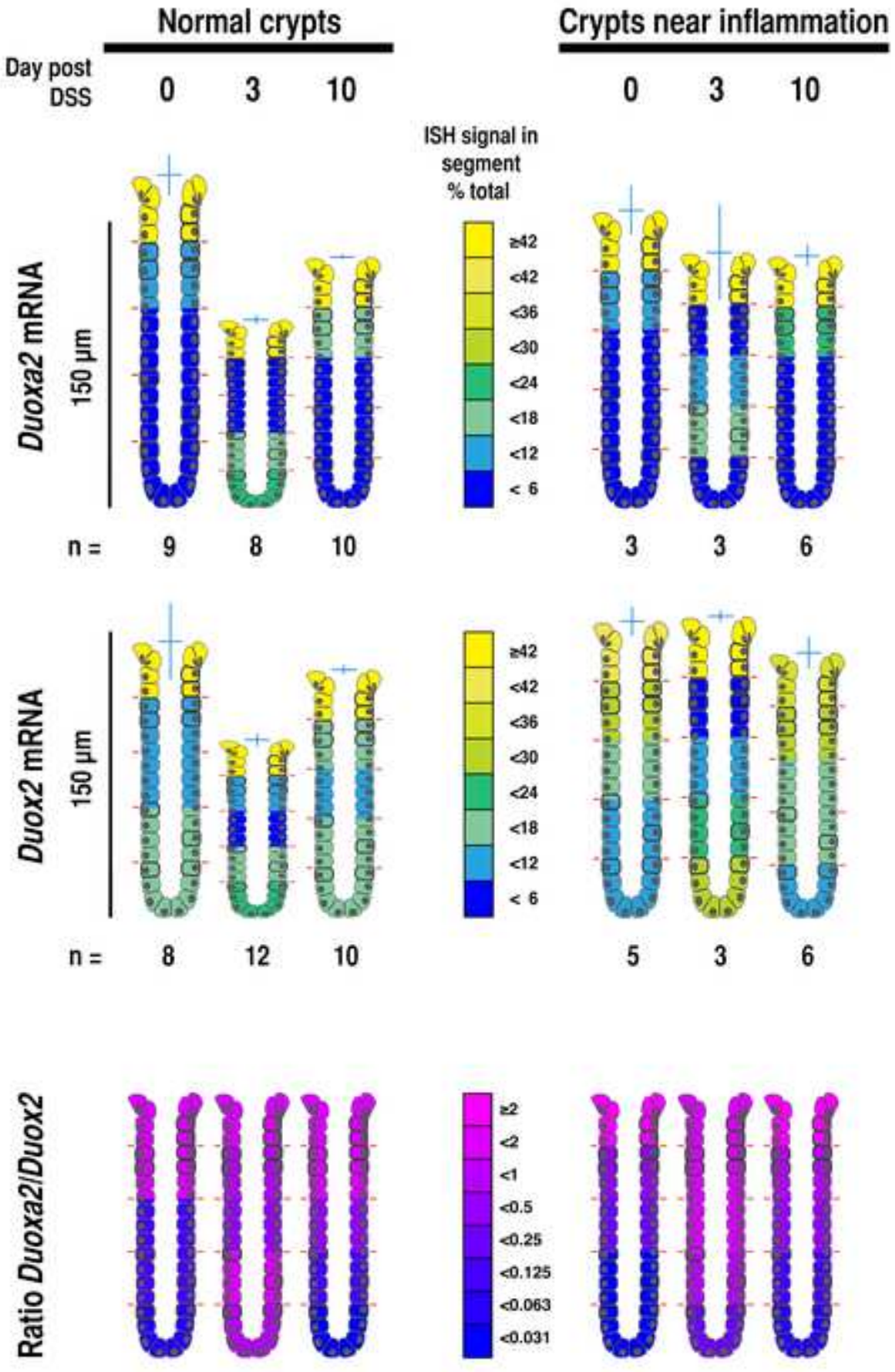

Figure 5

Click here to download Image Figure 5.tif

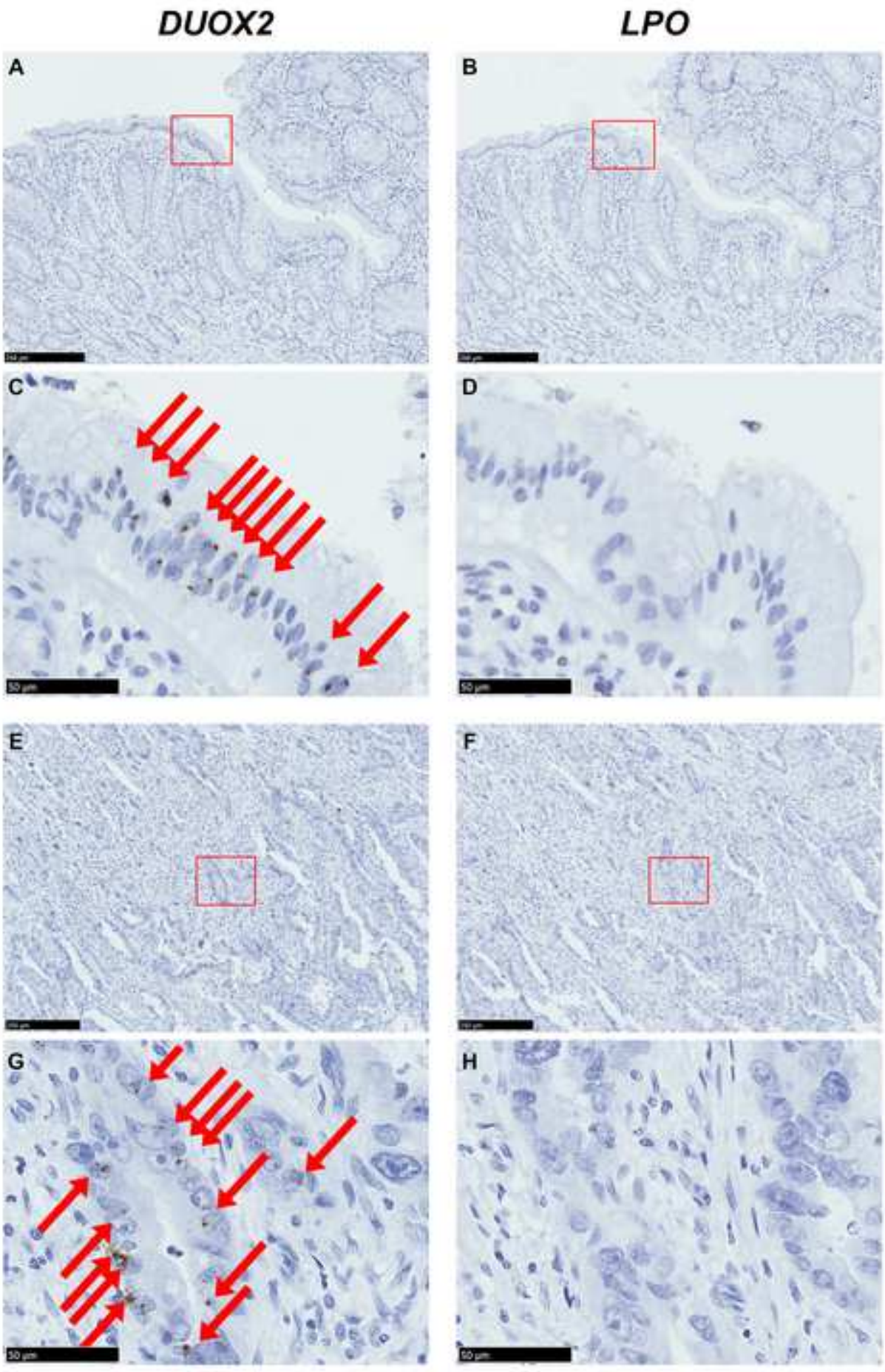

Figure 6

Click here to download Image Figure 6.tif

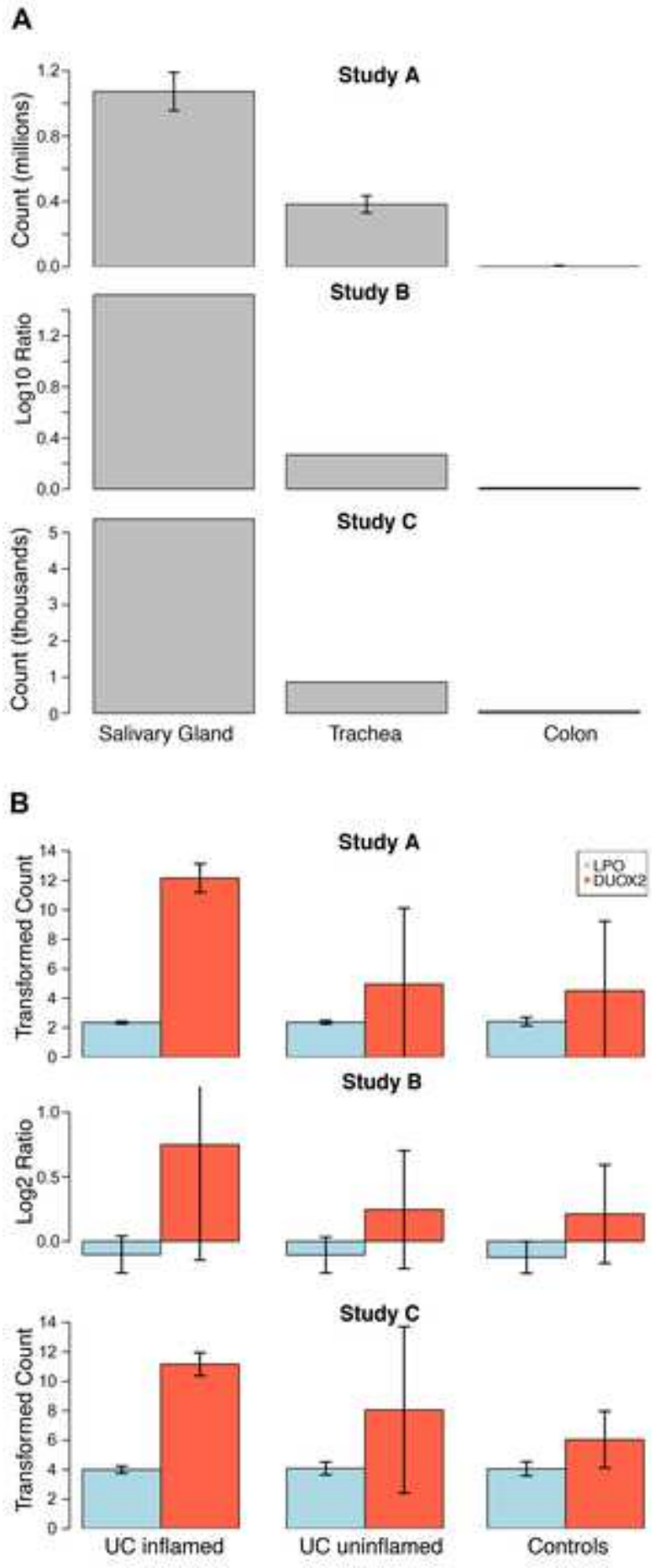

Supplemental digital content 1

Click here to download Supplementary Material For Review
Supplemental digital content 1.tif

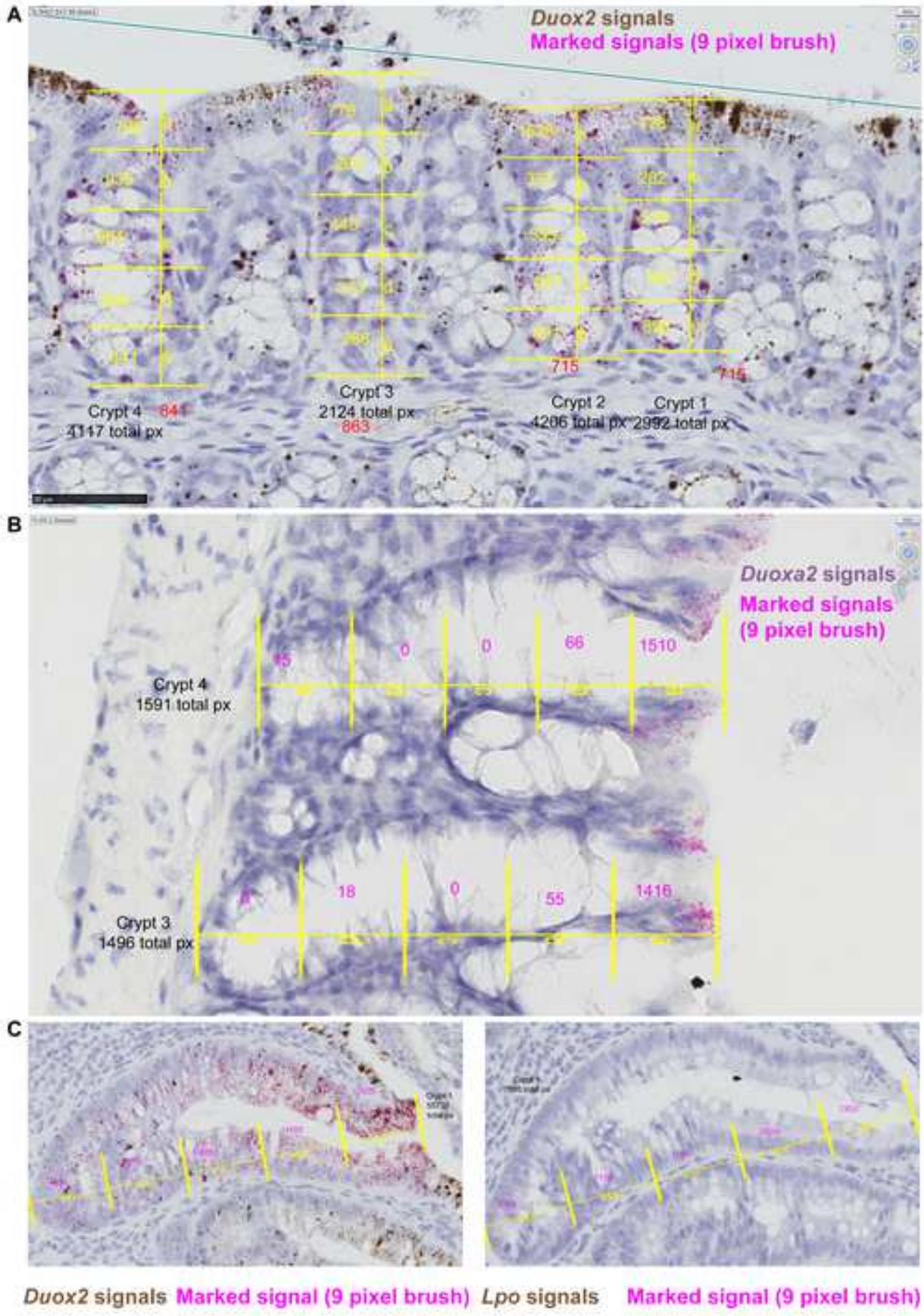

Supplemental digital content 2

Click here to download Supplementary Material For Review
Supplemental digital content 2.tif

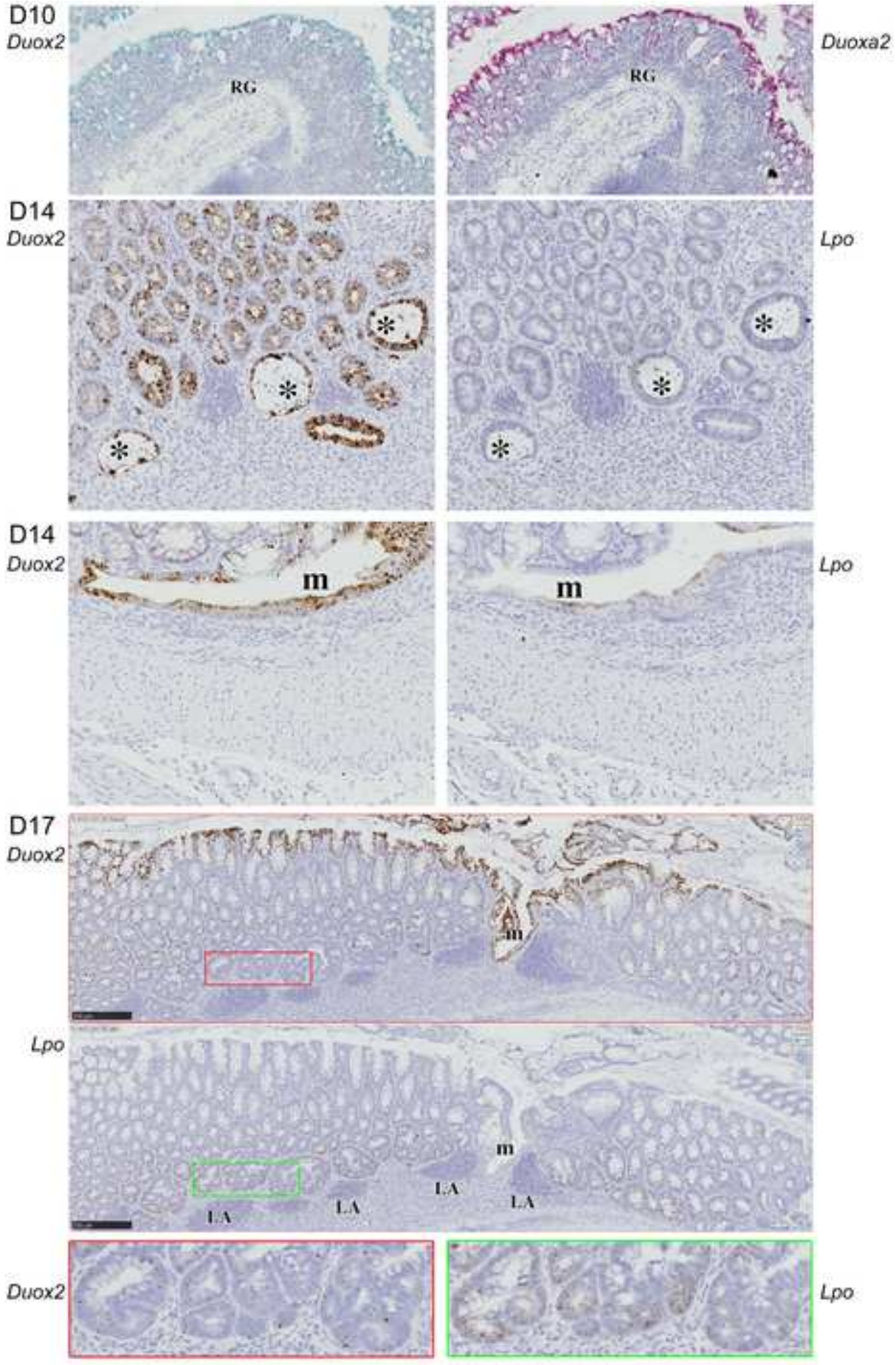

Supplemental digital content 3

Click here to download Supplementary Material For Review Supplemental digital content 3.tif

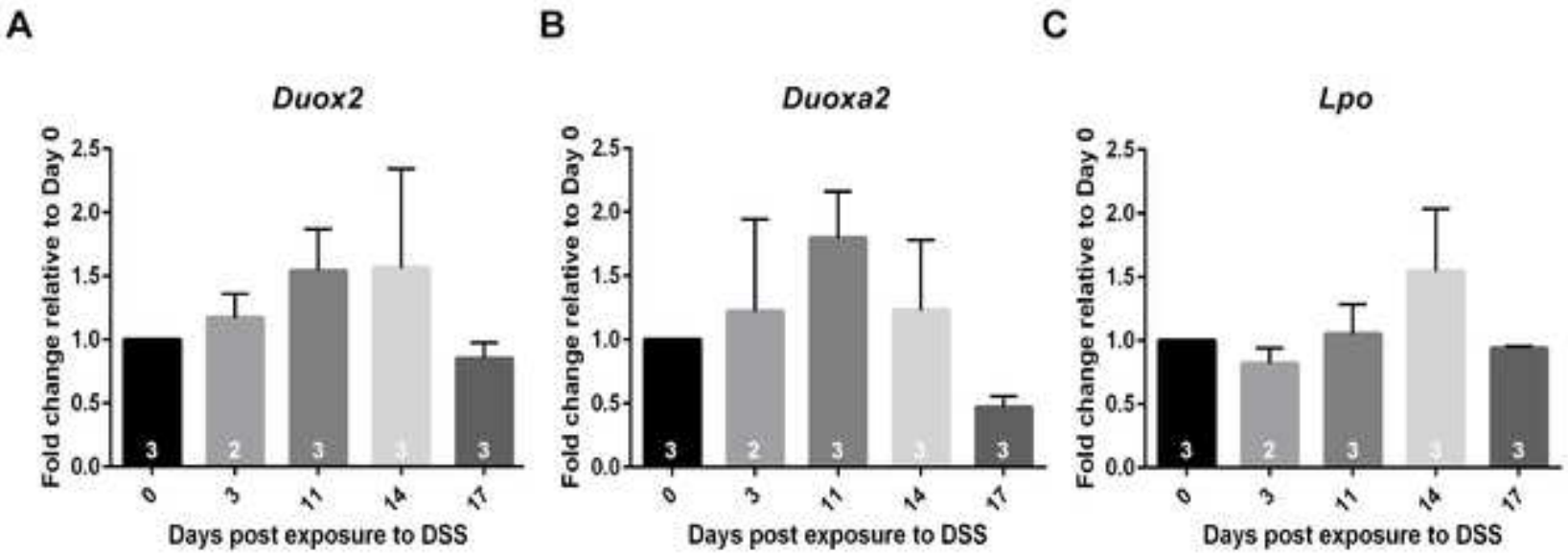

Supplemental digital content 4

Click here to download Supplementary Material For Review Supplemental digital content 4.tif

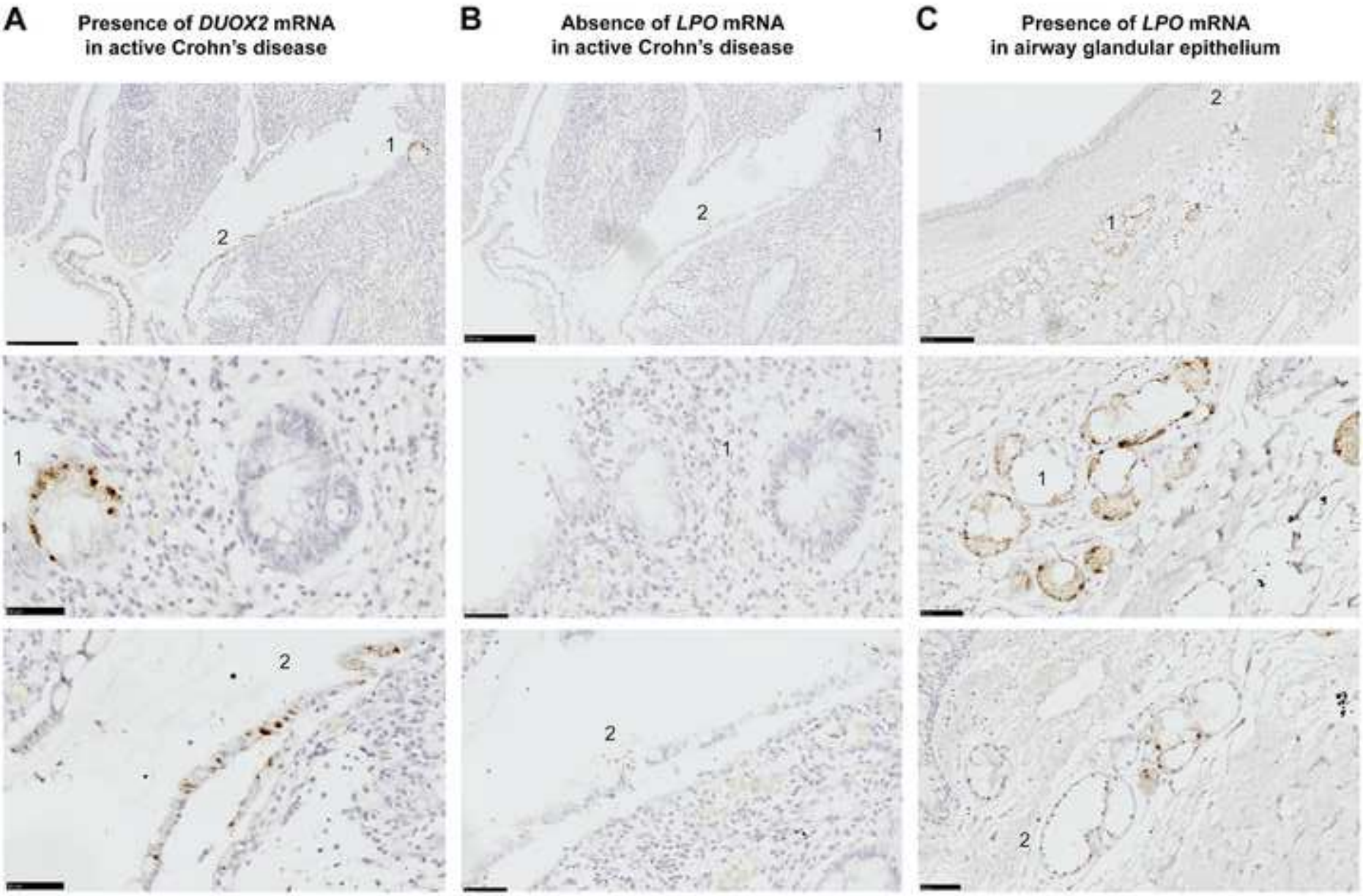

Supplemental digital content 5

Click here to download Supplementary Material For Review
Supplemental digital content 5.tif

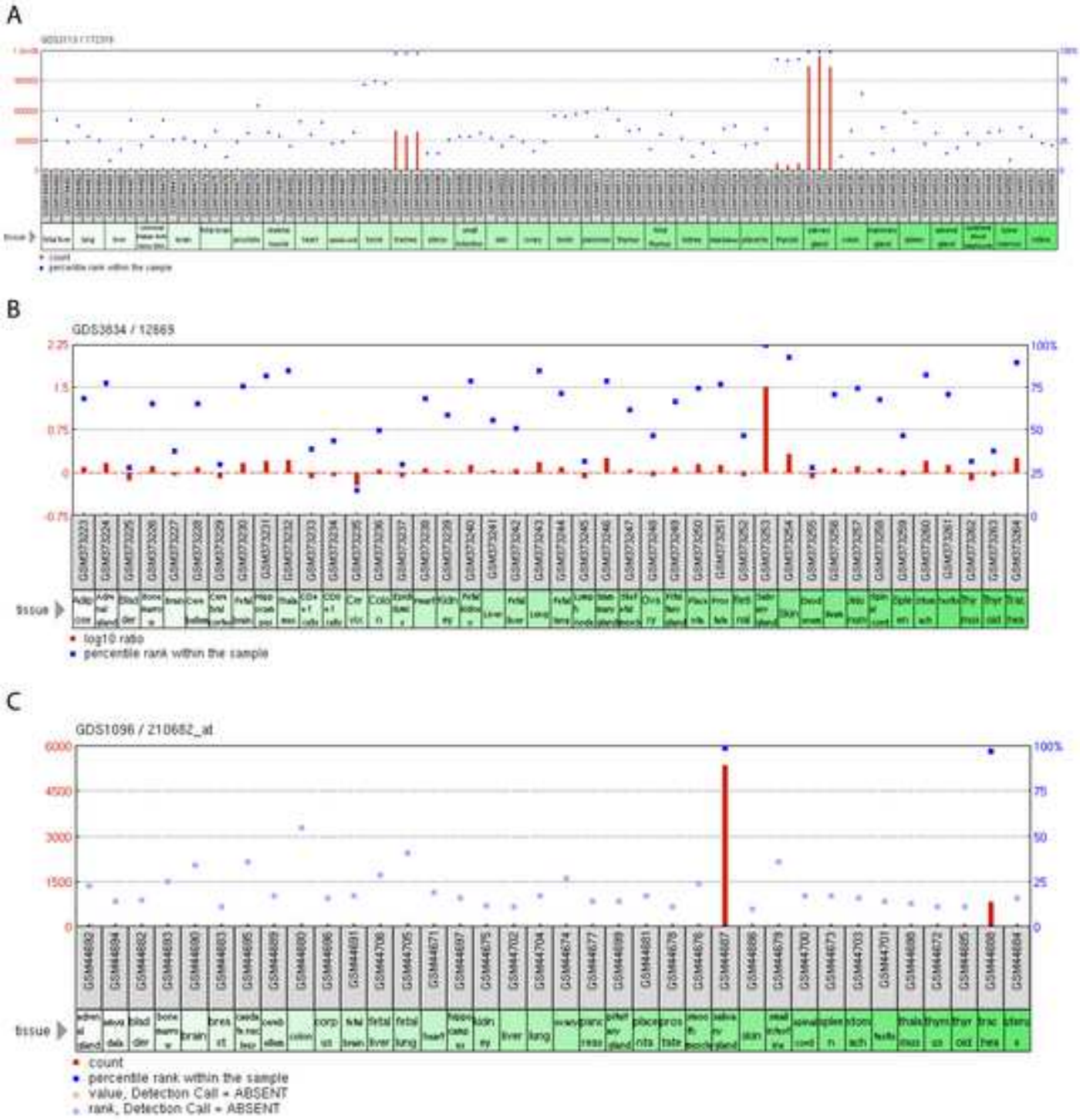

Supplemental digital content 6

Click here to download Supplementary Material For Review
Supplemental digital content 6.tif